AFRL-RV-PS-
TP-2015-0004

AFRL-RV-PS-
TP-2015-0004

TEMPERATURE DEPENDENCES FOR THE REACTIONS OF Ar^+, O_2^+, AND $C_7H_7^+$ WITH TOLUENE AND ETHYLBENZENE

Joshua J. Melko, et al.

01 July 2013

Journal Article

AIR FORCE RESEARCH LABORATORY
Space Vehicles Directorate
3550 Aberdeen Ave SE
AIR FORCE MATERIEL COMMAND
KIRTLAND AIR FORCE BASE, NM 87117-5776

REPORT DOCUMENTATION PAGE

Form Approved
OMB No. 0704-0188

1. REPORT DATE *(DD-MM-YYYY)*	**2. REPORT TYPE**	**3. DATES COVERED** *(From - To)*
01-07-2013	Journal Article	01 Feb 2013 - 02 May 2013

4. TITLE AND SUBTITLE
Temperature dependences for the reactions of Ar+, O_2+, and C_7H_7+ with toluene and ethylbenzene

5a. CONTRACT NUMBER

5b. GRANT NUMBER

5c. PROGRAM ELEMENT NUMBER
61102F

6. AUTHOR(S)
Joshua J. Melko, Shaun G. Ard, Nicholas S. Shuman, and Albert A. Viggiano

5d. PROJECT NUMBER
2303

5e. TASK NUMBER
PPM00004294

5f. WORK UNIT NUMBER
EF002012

7. PERFORMING ORGANIZATION NAME(S) AND ADDRESS(ES)
Air Force Research Laboratory
Space Vehicles Directorate
3550 Aberdeen Avenue SE
Kirtland AFB, NM 87117-5776

8. PERFORMING ORGANIZATION REPORT NUMBER
AFRL-RV-PS-TP-2015-0004

9. SPONSORING / MONITORING AGENCY NAME(S) AND ADDRESS(ES)

10. SPONSOR/MONITOR'S ACRONYM(S)
AFRL/RVBXT

11. SPONSOR/MONITOR'S REPORT NUMBER(S)

12. DISTRIBUTION / AVAILABILITY STATEMENT
Approved for public release; distribution is unlimited. (377ABW-2013-0384 dtd 14 May 2013)

13. SUPPLEMENTARY NOTES
Accepted for publication in the International Journal of Mass Spectrometry: 21 June 2013. Government Purpose Rights.

14. ABSTRACT

We have studied the reactions of Ar+, O-2(+), and C2H2* with toluene (CH3-C6H5) and ethylbenzene (C2H5-C6H5) as a function of temperature. Ar+ reacts with C7H8 at the collision rate constant at both 300 and 500 K to produce mainly C7H7+ cations (similar to 85%), with the remainder of the reactivity divided into numerous small channels. The fraction of C7H7+ produced as benzylium(+) (6 membered ring, Bz(+)) as opposed to tropylium(+) (7 membered ring, Tr+) is determined through ion-molecule reactivity to be primarily Bz(+). The reaction of Ar+ with C8H10 proceeds at slightly lower than the collision rate constant at 300 K, but increases to the collision rate constant at 500 K. Over 80% of the products were C7H7+, the large majority of which also is Bz(+). The O-2(+) reaction with Csflio proceeds at the collision rate constant and produces C8H10+, C6H6+, and C7H7+, with the latter again primarily being Bz(+). C7H7+ was found to react with both CH3-C6H5 and C2H5-C6H5 by both collisionally stabilized clustering and a bimolecular reaction forming R-C6H4-CH2+. At 300 K the rate constants are about half of the collision rate constant and drop rapidly with temperature. About 2/3 of the products are clusters at 300 K, 1/3 at 400 K, and negligible amounts at 500 and 600 K. Evidence for thermal dissociation of the cluster is presented. Calculations show the most stable structure is the one where the methylene group of benzylium is coordinated at the para position of the alkylbenzene, with one phenyl group approximately 45 degrees out of plane relative to the other. A bond strength of 15-16 kcal mol(-1) is calculated for both neutrals. Numerous less stable structures were found.

15. SUBJECT TERMS
Ion-Molecule Reactions; Pi-Pi-Interactions; Flowing Afterglow; Charge-Transfer; Gas-Phase; Electronic-Structure; Mass-Spectrometry; Gaseous Benzene; Tropylium Ion; Cations

16. SECURITY CLASSIFICATION OF:			**17. LIMITATION OF ABSTRACT**	**18. NUMBER OF PAGES**	**19a. NAME OF RESPONSIBLE PERSON**
					Dr. Raymond Bemish
a. REPORT	**b. ABSTRACT**	**c. THIS PAGE**			**19b. TELEPHONE NUMBER** *(include area code)*
Unclassified	Unclassified	Unclassified	Unlimited	10	

International Journal of Mass Spectrometry 353 (2013) 60–66

Contents lists available at ScienceDirect

International Journal of Mass Spectrometry

journal homepage: www.elsevier.com/locate/ijms

Temperature dependences for the reactions of Ar^+, O_2^+, and $C_7H_7^+$ with toluene and ethylbenzene

Joshua J. Melko, Shaun G. Ard, Nicholas S. Shuman, Albert A. Viggiano*

Air Force Research Laboratory, Space Vehicles Directorate, Kirtland AFB, NM 87117-5776, USA

ARTICLE INFO

Article history:
Received 17 May 2013
Received in revised form 21 June 2013
Accepted 21 June 2013
Available online 1 July 2013

Keywords:
Flow-tube
Kinetics
Alkylbenzenes
Rate constants

ABSTRACT

We have studied the reactions of Ar^+, O_2^+, and $C_7H_7^+$ with toluene (CH_3–C_6H_5) and ethylbenzene (C_2H_5–C_6H_5) as a function of temperature. Ar^+ reacts with C_7H_8 at the collision rate constant at both 300 and 500 K to produce mainly $C_7H_7^+$ cations (~85%), with the remainder of the reactivity divided into numerous small channels. The fraction of $C_7H_7^+$ produced as benzylium$^+$ (6 membered ring, Bz^+) as opposed to tropylium$^+$ (7 membered ring, Tr^+) is determined through ion-molecule reactivity to be primarily Bz^+. The reaction of Ar^+ with C_8H_{10} proceeds at slightly lower than the collision rate constant at 300 K, but increases to the collision rate constant at 500 K. Over 80% of the products were $C_7H_7^+$, the large majority of which also is Bz^+. The O_2^+ reaction with C_8H_{10} proceeds at the collision rate constant and produces $C_8H_{10}^+$, $C_6H_6^+$, and $C_7H_7^+$, with the latter again primarily being Bz^+. $C_7H_7^+$ was found to react with both CH_3–C_6H_5 and C_2H_5–C_6H_5 by both collisionally stabilized clustering and a bimolecular reaction forming R–C_6H_4–CH_2^+. At 300 K the rate constants are about half of the collision rate constant and drop rapidly with temperature. About 2/3 of the products are clusters at 300 K, 1/3 at 400 K, and negligible amounts at 500 and 600 K. Evidence for thermal dissociation of the cluster is presented. Calculations show the most stable structure is the one where the methylene group of benzylium is coordinated at the para position of the alkylbenzene, with one phenyl group approximately 45° out of plane relative to the other. A bond strength of 15–16 kcal mol^{-1} is calculated for both neutrals. Numerous less stable structures were found.

1. Introduction

It has long been known that $C_7H_7^+$ exists as both six and seven member ring structures – benzylium (Bz^+) and tropylium (Tr^+), respectively [1–11]. These rather stable ions are formed in many ion-molecule reactions of alkylbenzenes, and the history of their study has been detailed elsewhere [1–13]. Bz^+ reacts with alkylbenzenes by reaction (1):

$$CH_2C_6H_5^+ + R\text{–}C_6H_5 \rightarrow CH_2C_6H_4\text{–}R^+ + C_6H_6 \quad (1a)$$

$$CH_2C_6H_5^+ + R\text{–}C_6H_5 + M \rightarrow CH_2C_6H_5(R\text{–}C_6H_5)^+ + M \quad (1b)$$

while Tr^+ is unreactive, providing a convenient way to determine how much of each isomer is present.

We have recently observed $C_7H_7^+$ while developing a new flowing afterglow Langmuir probe technique to study dissociative recombination (i.e. $AB^+ + e^- \rightarrow A + B$) [14]. This is a variation of the variable electron and neutral density attachment mass spectrometry (VENDAMS) approach to studying a wide variety of previously inaccessible areas of plasma kinetics [15]. In this technique, Ar^+ is allowed to react with a neutral (e.g. toluene) to form one or more polyatomic ions. The ratios of Ar^+ to product cations are monitored as a function of the initial plasma density. Because Ar^+ does not recombine with e^-, but the polyatomic ions do, at higher plasma densities the Ar^+ to product ion ratio increases; analysis of the shape of the curve describing this behavior yields the rate constants for dissociative recombination of the various cations. In our initial paper on dissociative recombination [14], we chose toluene (C_7H_8) as one of the neutrals, which produces $C_7H_7^+$ as the major product. However, in those experiments we were unable to determine the ratio of Bz^+/Tr^+. In the present work we have examined the reaction of Ar^+ with toluene as a function of temperature in order to determine the Bz^+/Tr^+ product ratios. We have also expanded the work to include ethylbenzene, in part for future dissociative recombination studies. As a check, we have studied O_2^+ with ethylbenzene to compare to previous experiments [16]. Further, we have studied the Bz^+ reaction with both toluene and ethylbenzene, as our modeling relies on this secondary chemistry. Since Bz^+ clusters to both toluene and ethylbenzene at the pressures used in our experiments, calculations of the cluster bond strengths for reaction (1b) have

* Corresponding author. Tel.: +1 505 853 3399.
E-mail addresses: afrl.rvborgmailbox@kirtland.af.mil, albert.viggiano@us.af.mil (A.A. Viggiano).

1387-3806/$ – see front matter © 2013 Elsevier B.V. All rights reserved.
http://dx.doi.org/10.1016/j.ijms.2013.06.017

also been made. Considerable insight into the reaction mechanism is obtained from the measurements, calculations, and comparisons to previous data.

2. Experimental and theoretical methods

The experiments were performed in the AFRL variable temperature selected ion flow tube (SIFT). The instrument has been well described previously [17], and only details important to the present measurements are given. Ions are made in a high pressure ion source through electron impact. Pure Ar and O_2 were used to make Ar^+ and O_2^+, respectively. A mixture of Ar and C_7H_8 was used to make $C_7H_7^+$ in the source, which was determined to be 20–30% Tr^+ with the remainder Bz^+. The ions are extracted and injected into a quadrupole mass filter and the desired mass ion was selected. The ions enter the flow tube through a Venturi inlet and are carried downstream by a helium buffer. After several milliseconds and approximately 10^4–10^5 collisions with helium, C_7H_8 or C_8H_{10} was added through a finger inlet. Reactions occurred over the remaining 59 cm of the flow tube, and subsequently the flow was sampled through a small orifice in a rounded nose cone. The remainder of the flow was pumped away through a MKS servo-controlled gate valve, which maintained a controlled pressure within the flow tube. Sampled ions were then injected into a second quadrupole mass spectrometer and detected by a discrete dynode particle multiplier. The entire flow tube can be heated by resistance heaters in several zones. Here, most of the measurements were only done at 300 K and 500 K because the temperature dependence is weak. The exception is the work on $C_7H_7^+$, for which the temperature dependences are strong.

All flows were measured using MKS mass flow controllers. The ion velocity was calculated from the helium flow velocity and a previously measured ion to helium velocity ratio of ~1.6 [18]. Coupled with the known reaction length of 59 cm, this yields the reaction time. Rate constants were obtained by monitoring the primary decay as a function of added neutral concentration in the flow tube. For Ar^+ and O_2^+, single exponential decays were found and rate constants obtained in the normal fashion. For $C_7H_7^+$, the decays were fit to an exponential plus a constant functional form. The decaying portion was due to the Bz^+ reactions and the constant was attributed to Tr^+.

Toluene and ethylbenzene were introduced both neat and as mixtures in helium. The total count rate was largely independent of the extent of reaction, indicating minimal mass discrimination in the data, and no correction was needed. Branching ratios (without distinguishing between $C_7H_7^+$ isomers) were determined from the early part of the decay in the normal SIFT manner of extrapolating product branching fractions to zero flow. Anderson et al. showed that as long as the amount of primary ion depletion was kept small, the technique yields nascent branching ratios to within a few percentage points [19]. Alternatively, we iteratively solve the set of coupled differential equations describing the reaction scheme throughout the known reaction time, comparing the calculated product ion abundances to those measured through a weighted least squares fit [15]. By varying all relevant rate constants through a Monte Carlo procedure, over ranges constrained either by the literature or calculated collision rate constants, the full parameter space may be efficiently sampled. The latter analysis was done mainly to determine the Bz^+/Tr^+ ratio. The best fit value of the rate constant for each reaction channel is determined by identifying the minimum in the least squares parameter as a function of that rate constant; uncertainties are determined by values at the largest least squares parameter that still provide an acceptable description of the data. We find good agreement in product branching ratios determined using the two methods.

Errors for the linear decay rate constants are ±25% for absolute values and ±15% for relative changes as a function of temperature. The error in branching is estimated to be 5–10 percentage points for the large channels and 1–2 percentage points for the small channels. For the Bz^+ reactions errors are larger and are discussed in Section 3.4. We estimate that the Bz^+ and Tr^+ branching are accurate to 10 percentage points.

Calculations of the Bz^+-toluene and Bz^+-ethylbenzene cluster bond strengths were performed within the Gaussian 09W package at the B3LYP/6–311 + G(d) level [20–22]. Several starting geometries were explored, including geometries found in the literature for similar cluster ions [23–27]. Each optimized structure was confirmed as a true minimum via a frequency analysis. All clusters possess singlet ground state structures, and energies we provide include zero-point corrections.

3. Results and discussion

3.1. Reactions of O_2^+ with C_8H_{10}

As a test of the system, we have repeated our previous work on the reaction of O_2^+ with C_8H_{10}. The results are compared in Table 1. The rate constants are near the collision rate constant (within ~10%) and in good agreement with several previous measurements [16,28,29]. The branching measurements are generally in good agreement with previous measurements [6,16,28,29] with about 75% of the reactions producing $C_7H_7^+$, the bulk of the remainder being non-dissociative charge transfer, and finally 2–3% of $C_6H_6^+$. No clear trend with temperature is apparent; the small changes are within our estimated error. Less non-dissociative charge transfer was found at high temperature, as one would expect, but the observed change is within our error. The division of $C_7H_7^+$ into Bz^+ and Tr^+ is in excellent agreement with the ICR values in Fridgen et al. [6] and reasonable agreement with the SIFT values in that paper. Poorer agreement is found with the ratio reported by Arnold et al. [28]. The present measurements employed different methods of extracting the Bz^+/Tr^+ ratio than that used in the previous SIFT experiments. The present measurement and the ICR values of Fridgen et al. have a lower contribution from Tr^+ than the previous SIFT measurements. The agreement between the current study and Fridgen et al. [6], as well as the detailed statistical analysis performed here, lead us to favor the present results.

3.2. Reactions of Ar^+ with C_7H_8

Our results for the reaction of Ar^+ with C_7H_8 are listed in Table 2. The overall rate constant is within 6% of the collision rate constant [30] at both 300 and 500 K, well within our uncertainty. The vast majority of products are the two $C_7H_7^+$ cations (~85%). All product ions can be described as charge transfer, most of it dissociative; only about 2% of the non-dissociative channel is left after correcting the 92 amu peak for ^{13}C containing $C_7H_7^+$. Products with 4, 5, 6, and 7 carbons were found. The largest non-$C_7H_7^+$ cation is $C_5H_6^+$ at 3–4%. For reactions with known thermochemistry, the exothermicity is 64 kcal mol^{-1} and higher, so it is not surprising that dissociative charge transfer is the main process. About 2–3 times more Bz^+ is formed than Tr^+, with the former accounting for about 60% of the products at both temperatures and the latter 25%. While there is some scatter between the temperatures, it is hard to discern trends because many of the products are so small and their dependences are weak. Considering the exothermicity of the reaction, it is not surprising that relatively small amounts of added thermal energy have only a small effect.

Table 1
Product distributions and exothermicities for the reaction of O_2^+ with C_8H_{10} (ethylbenzene). Product distributions are corrected for isotopes, but not corrected for impurity ions from H_2O^+ or air related ions. The measured total rate constant and calculated collision rate constant [30] are shown at the bottom of the table. The error in branching is estimated to be 5–10 percentage points for the large channels and 1–2 percentage points for the small channels; measured rate constants have error bars of ±25%. Literature values are shown in brackets.

Products	Exothermicity (kcal mol^{-1})	300 K % branching [lit. values]	500 K % branching [lit. values]
$C_6H_6^+$	39.7	3 [3][a,b,c]	2 [2.5][b]
$C_7H_7^+$ (total)		71 [67][a,b] [61][c]	76 [75.5][b]
Bz^+	59.0	63 [44][a] [50][c] [64][d]	71
Tr^+	48.0	8 [23][a] [11][c] [7][d]	5
$C_8H_{10}^+$	76.3	25 [30][a,b] [36][c]	[20][b]
Total rate constant (cm^3 s^{-1}) [lit. values]		1.7×10^{-9} [1.7×10^{-9}][a] [2.2×10^{-9}][a,b]	1.6×10^{-9} [2.2×10^{-9}][b]
Collision rate constant (cm^3 s^{-1})		1.9×10^{-9}	1.9×10^{-9}

[a] Arnold et al. [28].
[b] Williams et al. [16] (average of two flow tube values, when appropriate).
[c] Fridgen et al. [6] SIFT measurement at 1 Torr.
[d] Fridgen et al. [6] ICR measurement, assumes total $C_7H_7^+$ is the current value of 71%.

Table 2
Product distributions and exothermicities for the reaction of Ar^+ with C_7H_8 (toluene). Product distributions are corrected for isotopes, but not corrected for impurity ions from H_2O^+ or air related ions. The measured total rate constant and calculated collision rate constant [30] are shown at the bottom of the table. The error in branching is estimated to be 5–10 percentage points for the large channels and 1–2 percentage points for the small channels; measured rate constants have error bars of ±25%.

Products	Exothermicity (kcal mol^{-1})	300 K % branching	500 K % branching
$C_4H_4^+$		0.6	1.5
$C_5H_4^+$		0.2	0.4
$C_5H_5^+$	64.1	1.5	2.5
$C_5H_6^+$	89.9	3.4	4.1
$C_6H_5^+$		2.1	3.2
$C_7H_5^+$		0.4	1.1
$C_7H_6^+$	100.5	2.0	2.0
$C_7H_7^+$ (total)		87.6	83.0
Bz^+	108.6	64	56
Tr^+	97.5	23	27
$C_7H_8^+$	160.0	2.0	2.2
Total rate constant (cm^3 s^{-1})		1.5×10^{-9}	1.5×10^{-9}
Collision rate constant (cm^3 s^{-1})		1.6×10^{-9}	1.6×10^{-9}

3.3. Reactions of Ar^+ with C_8H_{10}

Table 3 shows the results for Ar^+ with C_8H_{10}. The rate constants are near the collision rate constant at 500 K (95%), but not quite at the collision rate constant at 300 K (72%). This difference is outside our relative error and the unusual positive temperature dependence for a highly exothermic ion-molecule reaction was confirmed through several repeated measurements. Possibly the large energy mismatch between the Ar and C_8H_{10} ionization energies is responsible, resulting in curve crossings that are not completely favorable to charge transfer. The reaction proceeds entirely through dissociative charge transfer. This is in contrast to the O_2^+ reaction where a quarter of the reaction was non-dissociative. Again the large recombination energy of Ar^+ is almost certainly the reason. Just over 80% of the products are $C_7H_7^+$ at both temperatures. The remainder of the products are split nearly equally between $C_6H_6^+$ and $C_8H_9^+$. At 300 K, we find the Bz^+ to Tr^+ ratio to be about 8, in good agreement with Fridgen et al. [6] There was not enough curvature in the data at 500 K to obtain the Bz^+/Tr^+ ratio. However, based on the O_2^+ results, we do not expect much change from the 300 K result.

3.4. Reactions of Bz^+ with C_7H_8 and C_8H_{10}

The final reactions studied were Bz^+ with both C_7H_8 and C_8H_{10}. Both reactions involve the scheme detailed in Section 1, namely R and H transfer (1a) and association (1b). As shown later, the $Bz^+(R–C_6H_5)$ cluster bond strengths are rather small, indicating that the clusters are barely stable with respect to thermal dissociation at room temperature, and become increasingly unstable as the temperature is raised. Therefore, the complete reaction mechanism also involves the reverse of (1b), which is hidden in the data. Additionally, in an attempt to measure pressure dependences, it was found that the overall rate constants decreased slightly with pressure. This is not physical and indicates that the fragile species were partially dissociating due to the electric fields used in sampling. For these reasons, our uncertainties are larger than normal – we estimate the data are only accurate to a factor of two. However, the trends are so large the data are still informative.

Table 3
Product distributions and exothermicities for the reaction of Ar^+ with C_8H_{10} (ethylbenzene). Product distributions are corrected for isotopes, but not corrected for impurity ions from H_2O^+ or air related ions. The measured total rate constant and calculated collision rate constant [30] are shown at the bottom of the table. The error in branching is estimated to be 5–10 percentage points for the large channels and 1–2 percentage points for the small channels; measured rate constants have error bars of ±25%. Literature values are shown in brackets.

Products	Exothermicity (kcal mol^{-1})	300 K % branching	500 K % branching
$C_6H_6^+$	124.8	8	8
$C_7H_7^+$ (total)		81	84
Bz^+	167.2	72 [68][a]	[b]
Tr^+	156.1	9 [13][a]	[b]
$C_8H_9^+$	119.9	11	7
$C_8H_{10}^+$	161.4	[c]	[c]
Total rate constant (cm^3 s^{-1}) [lit. values]		1.3×10^{-9} [1.9×10^{-9}][a]	1.7×10^{-9}
Collision rate constant (cm^3 s^{-1})		1.8×10^{-9}	1.8×10^{-9}

[a] Fridgen et al. [6] ICR measurement, assumes total $C_7H_7^+$ is the current value.
[b] Not enough curvature for accurate determination.
[c] Too small to measure after correcting for $^{13}CC_7H_9^+$.

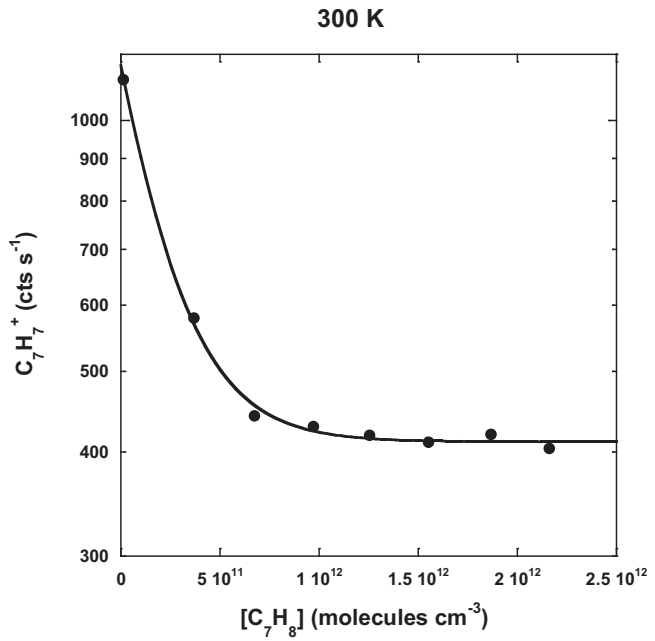

Fig. 1. Plot of $C_7H_7^+$ signal as a function of toluene concentration at 300 K. The fraction of $C_7H_7^+$ that declines is due to benzylium and the flat portion is due to tropylium.

Table 4
Rate constants and product distributions for the reaction of Bz^+ with C_7H_8 and C_8H_{10} at a number density of 3×10^{16} atoms cm^{-3} helium. The cluster product is shown in the table, the reactive fraction is the remainder. Branching and rate constants are accurate to a factor of two (see Section 3.4).

Temp (K)	C_7H_8		C_8H_{10}	
	k (cm^3 s^{-1})	Cluster (%)	k (cm^3 s^{-1})	Cluster (%)
300	7×10^{-10}	60	6×10^{-10}	68
400	4×10^{-10}	31	4×10^{-10}	30
500	1×10^{-10}	1	1×10^{-10}	1
600	3×10^{-11}	0	5×10^{-11}	1

Fig. 1 shows a decay of $C_7H_7^+$ as a function of C_7H_8 concentration at 300 K. The $C_7H_7^+$ initially declines and then levels out. The decline is due to reaction of Bz^+ and the flat portion is Tr^+. Typically about 1/3 of the ions were Tr^+. The rate constants are derived by fitting to an exponential plus a constant, and the line in Fig. 1 is the least squares fit. Because only a single species reacts, product branching can be deduced in the normal manner. Table 4 shows the rate constants and branching percentages for Bz^+ reacting with C_7H_8 and C_8H_{10} at a number density of 3×10^{16} atoms cm^{-3} helium. Overall rate constants decline sharply from 300 to 600 K, by factors of 23 and 12 for toluene and ethylbenzene, respectively. At 300 K, 60% and 68% of the reactivity with toluene and ethylbenzene, respectively, produces the cluster and the rate constants are a large fraction of the collision rate constant (~1/3). By 400 K, the rate constants drop by about 50%, as does the amount of clustering product. There is essentially no cluster left at 500 and 600 K (≤1%) and much greater reductions in the rate constants are found. The kinetics for the two reactions are similar, which is not surprising given the similarity between the neutral species. Thermal dissociation would normally show as curved decay plots. Since the data already have curvature due to the two isomers, it is not possible to quantify a second source of curvature and no information on the thermal dissociation rates was derived.

There have been several previous studies of the kinetics of Bz^+ reacting with C_7H_8, and one of Bz^+ reacting with C_8H_{10}. Dunbar [4] found only reaction 1a at 1.8×10^{-8} Torr, and determined a rate constant of 4×10^{-10} cm^3 s^{-1} for C_7H_8. Ausloos et al. [10] studied both the C_7H_8 and C_8H_{10} reactions at low pressure. They found values of 1.7×10^{-10} cm^3 s^{-1} and 5.7×10^{-10} cm^3 s^{-1}, respectively. In agreement with Dunbar, they observed only CH_2 transfer for the C_7H_8 reaction. Giardini-Guidoni and Zocchi [11] found a very small rate constant in a radiolysis experiment (2.1×10^{-11} cm^3 s^{-1}); this value is clearly an outlier. For the C_8H_{10} reaction, they found that ~3/4 of the reactions proceed by CH_2 transfer and 1/4 by a hydride transfer. For the C_7H_8 reaction, Sharma and Kebarle [7] found only clustering at 300 K and 4 Torr CH_4, and a faster rate constant of 2×10^{-9} cm^3 s^{-1}. At 436 K, they observed that the rate constant decreased substantially and that thermal dissociation occurred without any quantification given. Combining all the C_7H_8 data shows that the reaction is slower at lower pressures and produces only the CH_2 transfer product. In contrast, the rate constant increases to the collision rate constant at 4 Torr (CH_4) and produces only the cluster. The present result at 0.9 Torr helium is intermediate in both rate constant and branching. We did not see the hydride transfer channel for the C_8H_{10} reaction.

In order to understand the data, we have calculated the bond strengths of both Bz^+–C_7H_8 and Bz^+–C_8H_{10}. Numerous stable structures were found and Fig. 2 shows the structures and calculated stabilities. The most stable structure, shown at the bottom of the figure, is similar for both clusters. The methylene group of the benzylium structure is coordinated at the para position of the alkylbenzene, with one phenyl group approximately 45° out of plane relative to the other. We find the bond strengths for these structures are 15.2 and 15.8 kcal mol^{-1} for Bz^+–toluene and Bz^+–ethylbenzene, respectively. We refer to those as "para" in the figure. For C_7H_8, we found an "ortho" structure where the methylene of benzylium is coordinated at the ortho position of the alkylbenzene. This is only a couple of kcal mol^{-1} less stable than the "para" structure. No similar structure was found for C_8H_{10}, although it was searched for extensively.

The least stable structures found are the "stacked-same" structure (~5.5 kcal mol^{-1}) for both neutrals and the "stacked-opposite" structure for C_7H_8. These structures have the phenyl rings stacked, and the functional groups are on similar carbons ("same"), or opposite carbons ("opposite"), in their respective phenyl rings. The stacked opposite structure for C_8H_{10} is over twice as stable as that for C_7H_8. A similarly stable "stacked-opposite offset" structure was found for C_8H_{10}. "T-shape" structures, where the benzylium is slightly off-vertical relative to the horizontal alkylbenzene phenyl ring, were found to be almost as weakly bonded as the stacked-same structures (~5.8 kcal mol^{-1}).

In our flow tube only the most stable "para" structures are stable enough to survive the thousands of helium collisions [31,32]. To emphasize this point, we have calculated the energy distributions of the most stable Bz^+–C_7H_8 cluster at various temperatures. The results are shown in Fig. 3. The dashed vertical line represents the bond dissociation energy. At 300 K, most Bz^+–C_7H_8 molecules have energies below the dissociation energy (99%). Given the multi-collision effects in thermal dissociation, even at this temperature some thermal dissociation may be occurring. At 400 K, 30% of the molecules have enough energy to dissociate. While the reactive channel is roughly constant from 300 to 400 K (partial rate constant ~2.8×10^{-10} cm^3 s^{-1}), the partial rate constant for the clustering channel decreases by about a factor of 4. Some of that decrease is probably related to thermal decomposition affecting the decline in the Bz^+. At 500 K, there is essentially no cluster left; the partial rate constant drops by two orders of magnitude and 79% of the cluster has enough energy to dissociate. The reactive channel also drops by a factor of three. The trends continue at 600 K: no association

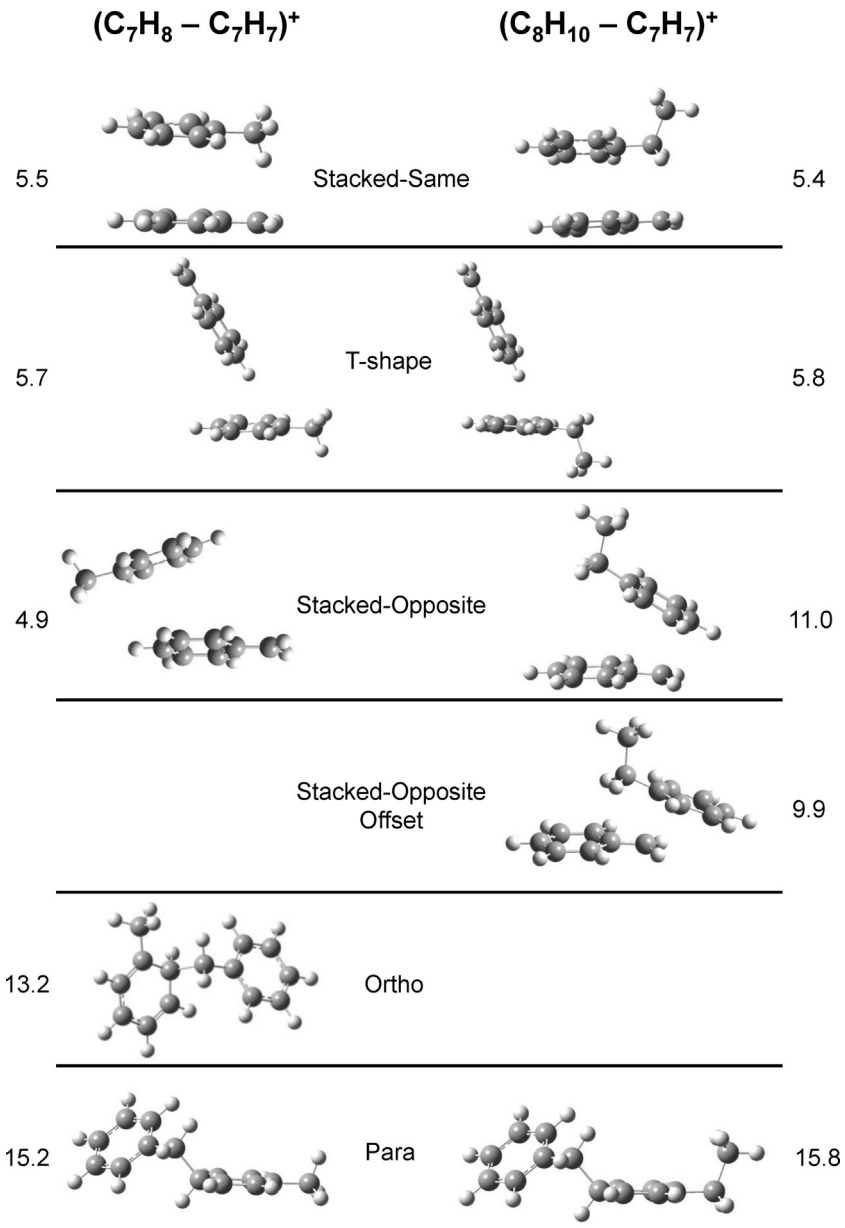

Fig. 2. Optimized geometries of the isomers for the benzylium–toluene (C_7H_8–$C_7H_7^+$, left) and benzylium–ethylbenzene (C_8H_{10}–$C_7H_7^+$ right) clusters. Carbon atoms and hydrogen atoms are gray and white, respectively. Numbers are the bond strengths in kcal mol^{-1}.

product was found and the reactive channel decreased by another factor of three. The steepness of the temperature dependence of the clustering channel is much larger than can be expected without consideration of thermal dissociation.

The 400–600 temperature dependence of the reactive channel is also large, suggesting a more complicated mechanism involving thermal activation. An example of this has been seen by our group previously [33]. At 300 K, $Cl^-(H_2O)$ reacts with CH_3Br to produce almost exclusively Br^-. That is an endothermic channel. At lower temperatures, $Cl^-(CH_3Br)$ was observed, showing that the reaction proceeded by a very slightly endothermic ligand switching to form $Cl^-(CH_3Br)$, which then underwent thermal activation to form Br^- in competition with Cl^- formation.

We speculate that a similar mechanism occurs here. The complete mechanism would then include the following steps. First, a complex is made.

$$^+CH_2{-}C_6H_5 + R{-}C_6H_5 \rightarrow (CH_2{-}C_6H_5{-}R{-}C_6H_5)^{+*} \quad (3)$$

The fact that 4 Torr of CH_4 is enough to completely stabilize the complex at 300 K and 0.9 Torr Helium only partially stabilizes it indicates that the complex lifetime is on the order of the helium collision time (i.e. about 10^{-7} s). The reactive channel must also be this slow or it would occur before the complex can be stabilized. The excited complex can then either dissociate (-3), go to products via transfer of the R-group (4), or be stabilized (5).

$$(CH_2{-}C_6H_5{-}R{-}C_6H_5)^{+*} \rightarrow {}^+CH_2{-}C_6H_5 + R{-}C_6H_5 \quad (-3)$$

$$(CH_2{-}C_6H_5{-}R{-}C_6H_5)^{+*} \rightarrow {}^+CH_2{-}C_6H_4{-}R + C_6H_6 \quad (4)$$

$$(CH_2{-}C_6H_5{-}R{-}C_6H_5)^{+*} + He \rightarrow (CH_2{-}C_6H_5{-}R{-}C_6H_5)^+ + He \quad (5)$$

Additionally, the stable complex can be activated, particularly at high temperatures

$$(CH_2{-}C_6H_5{-}R{-}C_6H_5)^+ + He \rightarrow (CH_2{-}C_6H_5{-}R{-}C_6H_5)^{+*} + He \quad (-5)$$

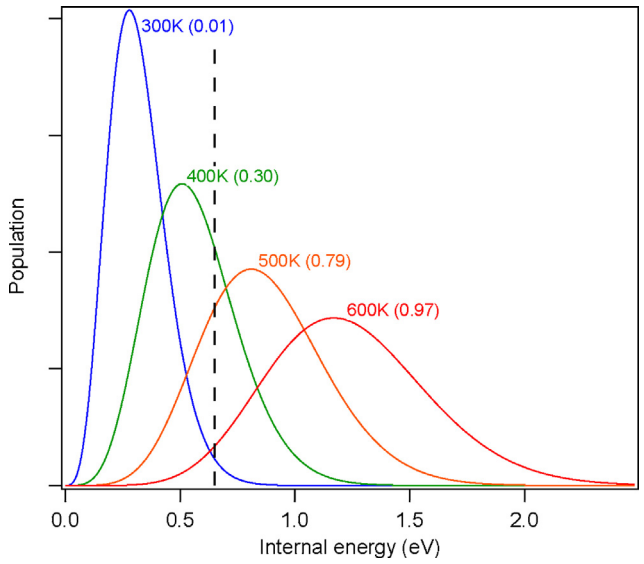

Fig. 3. Calculated thermal energy distributions of the Bz^+-C_7H_8 "para" cluster at the indicated temperatures. The bond dissociation energy (BDE, 15.2 kcal mol^{-1}) is indicated by the vertical line, and the fraction of each distribution above the BDE is indicated in parentheses.

At that point, reactions (-3), (4), and (5) occur. The thermally activated reactive channels, reaction (-5) followed by reaction (4), are calculated to be 7.8 and 7.6 kcal mol^{-1} endothermic for the most stable isomers. These are considerably lower in energy than the simple cluster dissociations represented by reactions (-5) followed by (-3), which are about 15 kcal mol^{-1} endothermic. A considerably high transition state barrier along the path of (-5), (4) could alter the conclusion, but locating that stationary point is beyond the scope of this work.

4. Conclusions

We have explored several aspects of the reactivity involving toluene, ethylbenzene, and $C_7H_7^+$. Reactions of Ar^+ with toluene and ethylbenzene have been probed to determine the ratio of benzylium to tropylium. The results show that mainly Bz^+ is formed, in addition numerous minor products were observed. Very little dependence on temperature was found, probably because the charge transfer energy is so large. Similarly, we explored the O_2^+ reaction with ethylbenzene and helped solve a previous discrepancy in the amount of Tr^+ formed. Finally, we explored temperature dependences of the reactions of Bz^+ with toluene and ethylbenzene. Combining our results at 0.9 Torr helium with previous studies at both higher and lower pressure shows that the reaction is complex, involving clustering, R-group transfer, and thermal activation.

Acknowledgments

We are grateful for the support of the Air Force Office of Scientific Research for this work under Project AFOSR-2303EP. J.J.M. and S.G.A. acknowledge the support of the National Research Council.

References

[1] E.-L. Zins, C. Pepe, D. Schroeder, Methylene-transfer reactions of benzylium/tropylium ions with neutral toluene studied by means of ion-trap mass spectrometry, Faraday Discussions 145 (2010) 157–169.
[2] D. Kuck, Mass spectrometry of alkylbenzenes and related compounds. Part I. Gas-phase ion chemistry of alkylbenzene radical cations, Mass Spectrometry Reviews 9 (1990) 187–233.
[3] C. Lifshitz, Tropylium ion formation from toluene, Accounts of Chemical Research 27 (1994) 138–144.
[4] R.C. Dunbar, Nature of the $C_7H_7^+$ ions from toluene parent ion photodissociation, Journal of the American Chemical Society 97 (1975) 1382–1384.
[5] P. Ausloos, Structure and isomerization of $C_7H_7^+$ ions formed in the charge transfer induced fragmentation of ethylbenzene, toluene, and norbornadiene, Journal of the American Chemical Society 104 (1982) 5259–5265.
[6] T.D. Fridgen, T.B. McMahon, J. Troe, A.A. Viggiano, A.J. Midey, S. Williams, Explaining Benzylium$^+$/Tropylium$^+$ yields from the fragmentation of Ethylbenzene$^+$, Journal of Physical Chemistry A 108 (2004) 5600–5609.
[7] D.K.S. Sharma, P. Kebarle, Stability and reactivity of the benzyl and tropylium cations in the gas phase, Canadian Journal of Chemistry 59 (1981) 1592–1601.
[8] P.N. Rylander, S. Meyerson, H.M. Grubb, Organic ions in the gas phase. II. The tropylium ion, Journal of the American Chemical Society 79 (1957) 842–846.
[9] S. Wexler, R.P. Clow, Ion-molecule reactions in gaseous benzene and toluene, Journal of the American Chemical Society 90 (1968) 3940–3945.
[10] P. Ausloos, J.-A.A. Jackson, S.G. Lias, Reactions of benzyl ions with alkanes, alkenes, and aromatic compounds, International Journal of Mass Spectrometry and Ion Physics 33 (1980) 269–283.
[11] A. Giardini-Guidoni, Z. Zocchi, Ion molecule reactions in gaseous benzene, toluene, and xylenes, Transactions of the Faraday Society 64 (1968) 2342–2347.
[12] C. Lifshitz, Y. Gotkis, J. Laskin, A. Ioffe, S. Shaik, Threshold formation of benzylium (Bz^+) and tropylium (Tr^+) from toluene. Nonstatistical behavior in Franck–Condon gaps, Journal of Physical Chemistry 97 (1993) 12291–12295.
[13] M. Malow, M. Penno, K.-M. Weitzel, The kinetics of methyl loss from ethylbenzene and xylene ions: the tropylium versus benzylium story revisited, Journal of Physical Chemistry 107 (2003) 10625–10630.
[14] J.A. Fournier, N.S. Shuman, J.J. Melko, S.G. Ard, A.A. Viggiano, A novel technique for measurement of thermal rate constants and temperature dependences of dissociative recombination: CO_2^+, CF_3^+, N_2O^+, $C_7H_8^+$, $C_7H_7^+$, $C_6H_6^+$, $C_6H_5^+$, $C_5H_6^+$, $C_4H_4^+$, and $C_3H_3^+$, Journal of Physical Chemistry 138 (2013) 154201.
[15] N.S. Shuman, T.M. Miller, A.A. Viggiano, J. Troe, Teaching an old dog new tricks: using the flowing afterglow to measure kinetics of electron attachment to radicals, ion–ion mutual neutralization, and electron catalyzed mutual neutralization, Advances in Atomic, Molecular, and Optical Physics 61 (2012) 209–294.
[16] S. Williams, A.J. Midey, S.T. Arnold, R.A. Morris, A.A. Viggiano, Y.-H. Chiu, D.J. Levandier, R.A. Dressler, M.R. Berman, Electronic, rovibrational, and translational energy effects in ion-aklybenzene charge-transfer reactions, Journal of Physical Chemistry A 104 (2000) 10336–10346.
[17] A.A. Viggiano, R.A. Morris, F. Dale, J.F. Paulson, K. Giles, D. Smith, T. Su, Kinetic energy, temperature and derived rotational temperature dependences for the reaction of $Kr^+(^2P_{3/2})$ and Ar^+ with HCl, Journal of Physical Chemistry 93 (1990) 1149–1157.
[18] P.M. Hierl, J.F. Friedman, T.M. Miller, I. Dotan, M. Mendendez-Barreto, J. Seeley, J.S. Williamson, F. Dale, P.L. Mundis, R.A. Morris, J.F. Paulson, A.A. Viggiano, A flowing afterglow apparatus for the study of ion-molecule reactions at high temperatures, Review of Scientific Instruments 67 (1996) 2142–2148.
[19] D.R. Anderson, V.M. Bierbaum, C.H. DePuy, J. Grabowski, Flowing afterglow studies of organic positive ions generated by penning ionization using metastable argon atoms, International Journal of Mass Spectrometry and Ion Processes 52 (1983) 65–94.
[20] W. Kohn, A.D. Becke, R.G. Parr, Density functional theory of electronic structure, Journal of Physical Chemistry 100 (1996) 12974–12980.
[21] C. Lee, W. Yang, R.G. Parr, Development of the Colle–Salvetti correlation-energy formula into a functional of the electron density, Physical Review B 38 (1988) 785–789.
[22] M.J. Frisch, G.W. Trucks, H.B. Schlegel, G.E. Scuseria, M.A. Robb, J.R. Cheeseman, G. Scalmani, V. Barone, B. Mennucci, G.A. Petersson, H. Nakatsuji, M. Caricato, X. Li, H.P. Hratchian, A.F. Izmaylov, J. Bloino, G. Zheng, J.L. Sonnenberg, M. Hada, M. Ehara, K. Toyota, R. Fukuda, J. Hasegawa, M. Ishida, T. Nakajima, Y. Honda, O. Kitao, H. Nakai, T. Vreven, J.A. Montgomery, J.E. Peralta, F. Ogliaro, M. Bearpark, J.J. Heyd, E. Brothers, K.N. Kudin, V.N. Staroverov, R. Kobayashi, J. Normand, K. Raghavachari, A. Rendell, J.C. Burant, S.S. Iyengar, J. Tomasi, M. Cossi, N. Rega, J.M. Millam, M. Klene, J.E. Knox, J.B. Cross, V. Bakken, C. Adamo, J. Jaramillo, R. Gomperts, R.E. Stratmann, O. Yazyev, A.J. Austin, R. Cammi, C. Pomelli, J.W. Ochterski, R.L. Martin, K. Morokuma, V.G. Zakrzewski, G.A. Voth, P. Salvador, J.J. Dannenberg, S. Dapprich, A.D. Daniels, Farkas, J.B. Foresman, J.V. Ortiz, J. Cioslowski, D.J. Fox, Gaussian 09, Revision B. 01, 2009, Wallingford, CT.
[23] E.C. Lee, D. Kim, P. Jurecka, P. Tarakeshwar, P. Hobza, K.S. Kim, Understanding of assembly phenomena by aromatic–aromatic interactions: benzene dimer and the substituted systems, Journal of Physical Chemistry A 111 (2007) 3446–3457.
[24] M.O. Sinnokrot, C.D. Sherrill, High-accuracy quantum mechanical studies of π–π interactions in benzene dimers, Journal of Physical Chemistry A 110 (2006) 10656–10668.
[25] A. Calderone, R. Lazzaroni, J.L. Brédas, Geometric and electronic structure of alkane/benzene, ethylbenzene/benzene, and alkane/ethylbenzene complexes: towards the characterization of polymer alloy composites, Synthetic Metals 95 (1998) 1–15.
[26] S. Tsuzuki, K. Honda, T. Uchimaru, M. Mikami, Ab initio calculations of structures and interaction energies of toluene dimers including CCSD(T) level electron correlation correction, Journal of Chemical Physics 122 (2005) 144323.
[27] T. Smith, L.V. Slipchenko, M.S. Gordon, Modeling π–π interactions with the effective fragment potential method: the benzene dimer and substituents, Journal of Physical Chemistry A 112 (2008) 5286–5294.

[28] S.T. Arnold, I. Dotan, S. Williams, A.A. Viggiano, R.A. Morris, Selected ion flow tube studies of air plasma cations reacting with alkylbenzenes, Journal of Physical Chemistry A 104 (2000) 928–934.
[29] A.I. Fernandez, A.A. Viggiano, A.I. Maergoiz, J. Troe, V.G. Ushakov, Thermal decomposition of ethylbenzene cations ($C_8H_{10}^+$): experiments and modeling of falloff curves, International Journal of Mass Spectrometry 241 (2005) 305–313.
[30] T. Su, W.J. Chesnavich, Parametrization of the ion-polar molecule collision rate constant by trajectory calculations, Journal of Chemical Physics 76 (1982) 5183–5185.
[31] S.T. Arnold, R.A. Morris, A.A. Viggiano, Competition between electron detachment and monomer evaporation in the thermal dissociation of hydrated electron clusters, Journal of Chemical Physics 103 (1995) 9242–9248.
[32] J.V. Seeley, R.A. Morris, A.A. Viggiano, Gas phase reactions of hydrated halides with chlorine, Journal of Physical Chemistry 100 (1996) 15821–15826.
[33] J.V. Seeley, R.A. Morris, A.A. Viggiano, H. Wang, W.L. Hase, Temperature dependencies of the rate constants and branching ratios for the reactions of $Cl^-(H_2O)_{0-3}$ with CH_3Br and thermal dissociation rates for $Cl^-(CH_3Br)$, Journal of the American Chemical Society 119 (1997) 577–584.

DISTRIBUTION LIST

DTIC/OCP
8725 John J. Kingman Rd, Suite 0944
Ft Belvoir, VA 22060-6218 1 cy

AFRL/RVIL
Kirtland AFB, NM 87117-5776 2 cys

Official Record Copy
AFRL/RVBXT/Dr. Raymond Bemish 1 cy